ce/papers
The online collection for conference papers in civil engineering
Ernst & Sohn A Wiley Brand

NORDIC STEEL 2019
The 14th Nordic Steel Construction Conference,
September 18–20, 2019, Copenhagen, Denmark

Automatically Welded Tubular X-Joints for Jacket Substructures

Prediction of the Technical Fatigue Crack Location

Peter Schaumann[a], Karsten Schürmann*[,a], Andreas Pittner[b], Michael Rethmeier[b,c]

[a] Leibniz University Hannover, Institute for Steel Construction – ForWind Hannover, Germany
schaumann@stahl.uni-hannover.de, schuermann@stahl.uni-hannover.de
[b] Federal Institute for Materials Research and Testing (BAM), Germany
andreas.pittner@bam.de, michael.rethmeier@bam.de
[c] Technical University of Berlin, Institute of Machine Tools and Factory Management, Germany

ABSTRACT

To increase the competitiveness of jacket substructures compared to monopiles a changeover from an individual towards a serial jacket production based on automated manufactured tubular joints combined with standardized pipes has to be achieved. Therefore, this paper addresses fatigue tests of automatically welded tubular X-joints focusing on the location of the technical fatigue crack. The detected location of the technical crack is compared to numerical investigations predicting the most fatigue prone notch considering the structural stress approach as well as the notch stress approach. Besides, the welding process of the automated manufactured tubular X-joints is presented.

Keywords: Tubular X-joints, fatigue tests, technical crack detection, local fatigue approaches

1 INTRODUCTION

Based on the German strategy of planning offshore wind farms outside the Wadden Sea National Park and as far away from the coastline as possible, most of the wind farms in Germany's Exclusive Economic Zone have water depths of around 35 m and more. In addition to (XL-) monopiles, resolved support structures such as jackets can be considered as foundation structures for these water depths. For example, 70 wind turbines of the 5 MW class were installed on jackets at a water depth of 37 - 43 m in the Viking wind farm located in the Baltic Sea.

Jacket foundation structures are designed as spatially resolved hollow section structures based on the construction of oil and gas platforms and are characterised by high rigidity with low material input. The spatial structure of the jacket is created with the typical tubular connection variants double-K-, X- and double-Y-joints.

Especially for jackets, the optimization potential for production and design is almost unused. An essential component of this optimization is the individual production of the tubular joints combined with the use of standardized pipes. This modular principle enables an automatic production of the tubular joints, which increases the competitiveness of the jackets especially against the background of the large quantities required for offshore wind farms (1).

2 AUTOMATED WELDING OF TUBULAR X-JOINTS

2.1 Weld seam preparation of the tubes

For the application of the automated welding procedure of tubular joints for offshore jacket substructures a scaled tubular X-joint (1 : 3.3) was designed within the German joint research project "FATInWeld" for test purposes. The geometry of the X-joint is presented within Fig. 1, left.

The design of the HV seam preparation along the three-dimensional intersection geometry of the X-joint was CAD-supported, Fig. 1, right. Care was taken to ensure that the cross-sectional areas in the range 45°-315° in direction of rotation (Fig. 2) were constant with a seam opening angle of 45°.

https://doi.org/10.1002/cepa.1140 wileyonlinelibrary.com/journal/cepa

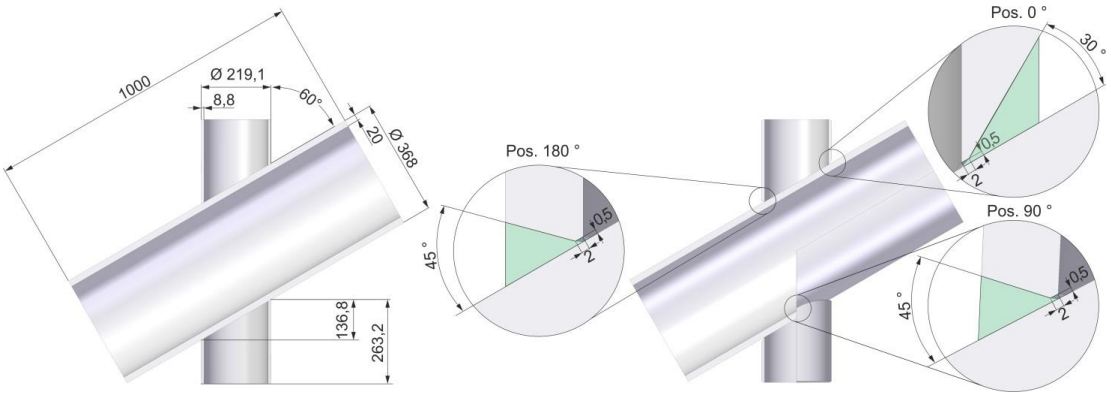

Fig. 1. Geometry definition and weld seam preparation for the automated welding of the tubular X-joints, (2)

In the 315°-45° range, the seam opening angle was continuously reduced to a minimum of 30° (position 0°).

Since deviations in diameter and wall thickness from the nominal values of the standard tubes lead to significant local deviations in the weld preparation the geometric tolerances of the chord and brace tubes are of high relevance. In order to minimize the deviations within the weld preparation, the tolerances of the tubes were recorded and individual CAD data was used for the manufacturing of the weld preparation. The seam preparation of the brace stub was then manufactured by milling.

2.2 Automated gas metal arc welding procedure

Due to the geometric tolerances of the standard tubes, the positioning was robot-supported using defined control measuring points for checking the axial alignment of the brace tubes (2). By applying this procedure an axial offset lower than 0.25 mm could be reached which is an acceptable value for the fatigue tests.

The welding process was designed on the basis of the seam preparation defined in Fig. 1, right. With regard to the material specifications the brace stubs were made of S355J2H according to DIN EN 10210-1 (3). The chord tubes were made of S355J2H with the additional quality Z35. A solid wire with a diameter of 1.2 mm of quality G 46 6 M21 3Ni1 according to ISO 14341 (4) was used as filler material. As shown in Fig. 2 a), the welding process starts at -45° (or 315°) with a linearly increased wire feed rate from 7.5 m/min to 11.5 m/min. The process parameters remain constant in the 45°-315° range. From the 315° position, the wire feed rate is reduced linearly to 8.5 m/min at 45° (or 405°). Related to the welded tubular X-joint, the 0° position corresponds to the crown heel, the 90° position belongs to the saddle and the 180° position corresponds to the crown toe.

The prediction of the fatigue strength considering the welding production chain is based on the evaluation of profile measurement data along the welding trajectory which is stored in a relational database (5). These 3D weld geometry measurement data obtained by laser scanning represent the actual transfer data to the simulation based analysis of the fatigue strength. Due to the automated GMA welding process, a seam transition with very mild notches could be achieved (2). This applies to the complete length of the weld seam trajectory. In addition, the fluctuation of the seam geometry between different tubular joints is very low, which guarantees a high reproducibility.

3 AXIAL FATIGUE TESTS ON ROBOT WELDED X-JOINTS

3.1 Test setup and procedure

Axial fatigue tests have been conducted on the automatically welded tubular X-joints using a servo-hydraulic 1 MN testing device. The tubular X-joint was adapted to the testing device with bolted ring flange connections combined with two adapters for the clamping jaws of the testing device, compare Fig. 3.

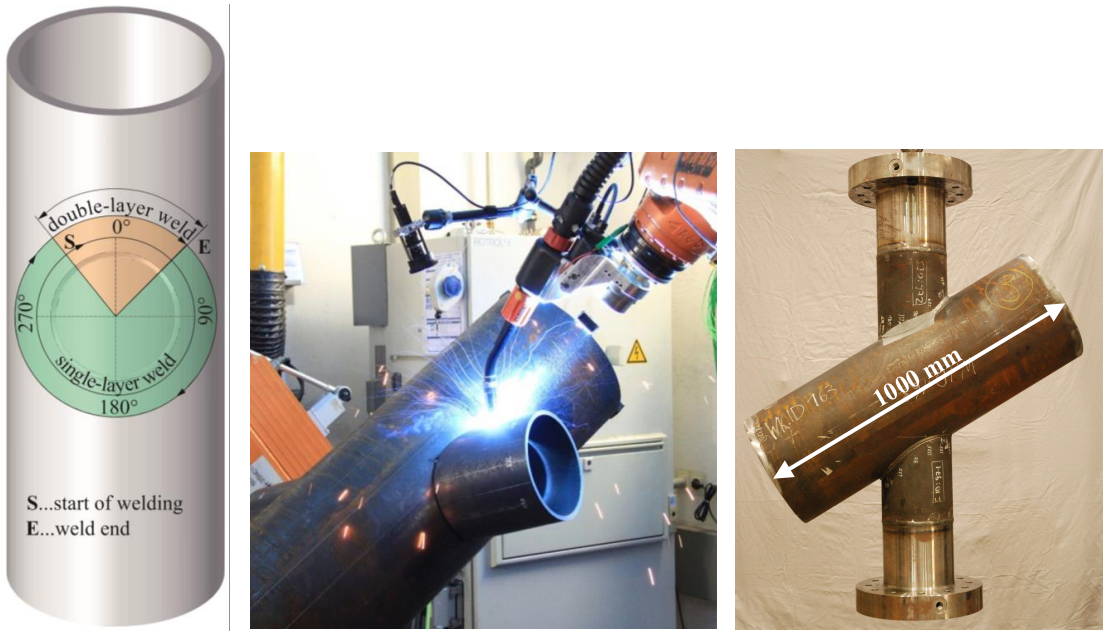

a) b) c)

Fig. 2. a) Setup of the gas metal arc welding process along the weld trajectory, (2); b) Automated welding of a tubular X-joint; c): Final geometry of the tubular X-joints with added ring flanges

Since the structural stress approach, which is the state of the art for the fatigue design of tubular joints, predicts the through thickness crack, this failure criteria is decisive for the testing of the tubular joints. During the tests the through thickness crack has been observed by detecting a change of inner pressure within the three pipes. Therefore, an overpressure has been applied within the two braces as well as a negative pressure within the chord.

For the determination of the technical crack location two ARAMIS 3D 12M digital image correlation (DIC) systems have been utilized. Periodically, at the maximum load a picture of the prepared hot spot was simultaneously taken by both ARAMIS systems. Therefore, the first system (the master system) was triggered directly by the load signal of the testing device. The second ARAMIS system (the slave system) was controlled by the master system by sending a trigger signal at each time a picture was taken.

The required high-contrast surface was obtained by applying a stochastic black-white speckle pattern using the white developer known from the dye penetrant inspection combined with sprayed liquid black graphite, Fig. 3. These coating substances were applied instead of corresponding lacquers to allow a crack opening of the coating after crack initiation within the specimen.

The fatigue tests have been performed considering a bottom to top load ratio of $R = 0.1$ with an axial top load of $F_{ax,o} = 390$ kN and a testing frequency of 5 Hz applying constant amplitude values.

3.2 Technical crack location

During the fatigue tests the axial strain ε_x perpendicular to the weld was measured using the ARAMIS systems. The results are presented in Fig. 4, whereby the axial strain distribution after $N = N_{tech.Crack}$ cycles is shown in part a). The distribution of ε_x for $N_{tech.Crack} < N < N_{through\ thickness}$ is presented in the part b).

The first axial strain hot spot and hence the location of the initial technical crack was detected within the chord sided notch close to the location of the saddle position between path 4 and 5 according to the paths definition given in Fig. 5, b). The crack was then growing along the notch towards both crown positions (heel and toe) resulting in a through thickness crack towards the chord. Additionally, it can be seen within Fig. 4 that no increased axial strain and hence no measurable damage occurred within the brace sided notch.

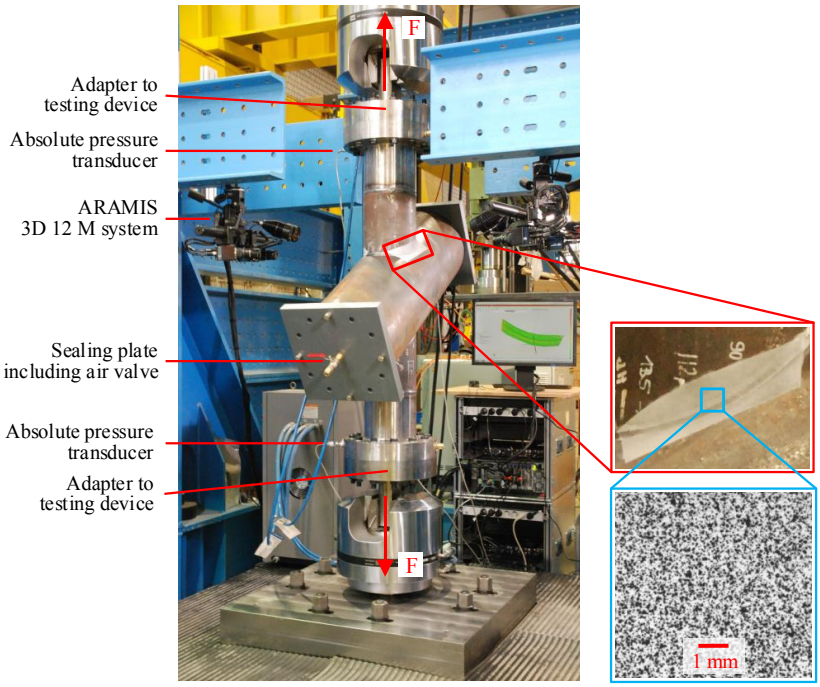

Fig. 3. Test setup of the axial fatigue tests including the stochastic black and white speckle pattern for the digital image correlation measurement

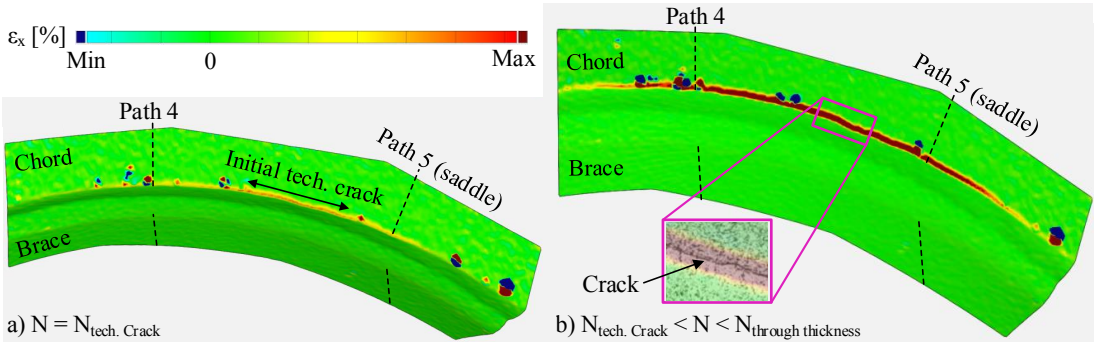

Fig. 4. Axial strain ε_x distribution measured by ARAMIS during the fatigue tests at the hot-spot location of the X-joint for $N = N_{tech.Crack}$ in part a) and for $N_{tech.Crack} < N < N_{through\ thickness}$ in part b). The initial technical crack occurred between path 4 and 5 which are defined in Fig. 5, b)

4 NUMERICAL INVESTIGATIONS

4.1 Application of the structural stress approach for the tubular X-Joint

For the application of the structural stress approach (SSA) according to the DNVGL-RP-C203 recommendation (6) a numerical model of the X-joint was generated by using the finite element software ANSYS 17.2. The weld seam geometry between the chord and the brace was based on the actual laser scanned weld geometry of the automatically welded tubular joint. 20-node solid elements (Solid 186) with quadratic shape functions were utilized considering linear elastic material behaviour (Young's modulus of E = 210,000 N/mm² and Poisson's ratio of ν = 0.3). The axial unit load F was applied on top of the upper brace whereas the lower brace was fixed, see Fig. 5, a). The stress concentration factors (SCF) were computed on behalf of nine paths for the chord and the brace around one half of the chord to brace intersection, see Fig. 5, b).

4.2 Application of the notch stress approach for the tubular X-Joint

For the application of the notch stress approach (NSA) according to the IIW recommendation (7) the submodeling technique was used due to the required mesh refinement within the fictitiously rounded weld notches, see Fig. 5, a). With regard to the nine extrapolation paths on the chord and the brace (see Fig. 5, b)) for the SSA, nine separate submodels were generated. These submodels represent similarly to the numerical model for the SSA application the actual laser scanned weld geometry of the tested tubular X-joints. The notch was meshed by using at least six finite elements along the rounded notch (Solid 187) depending on the actual geometry again with quadratic shape functions and linear elastic material behavior (E = 210,000 N/mm² and ν = 0.3). The load case was equivalent to the previously described load case for the SSA.

For the computation of the elastic fatigue notch factor K_f the maximum surface node value of the first principal stress σ_1 within the rounded notch was read out for each location of the nine corresponding paths of the brace and the chord. The K_f values were then transformed into equivalent SCF_{NSA} according to (8) to enable comparability between the results based on the NSA and the SCF values based on the SSA.

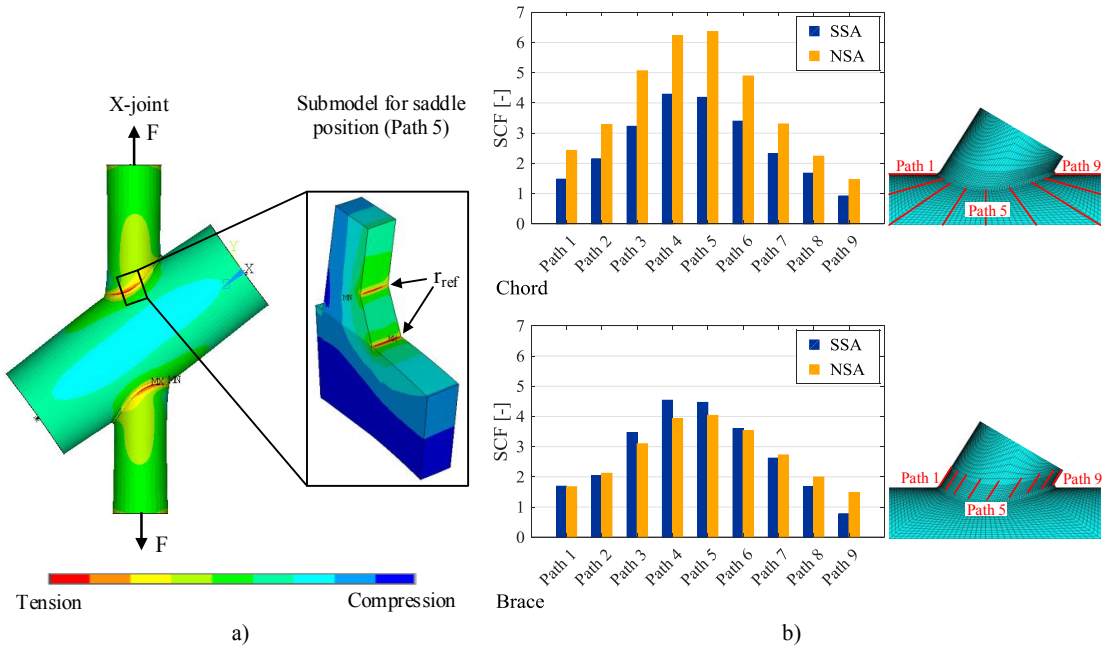

Fig. 5. a) Relative distribution of first principal stress σ_1 for the tubular X-joint as well as for the submodel of the saddle position for an axial unit load F, (8); b) Comparison of the SCFs for chord and brace based on the SSA as well as on the NSA. The corresponding path numbering is presented on the right

4.3 Comparing the applicability of SSA and NSA for the X-Joint

The resulting SCF values according to the numerical studies are presented in Fig. 5 b). Comparing these two diagrams a significant difference between the NSA and the SSA can be seen especially for the chord. The equivalent SCF_{NSA} values for the chord are significantly increased compared to both, the SCF_{NSA} values for the brace sided notch as well as the SCFs based on the SSA.

The differences between both approaches are due to the characteristics of the tubular X-joint. Due to the stiffness distribution between chord and brace, the axially loaded X-joint shows a structural hot spot within the brace at the saddle position which is decisive for the SSA. However, for the results based on the NSA the characteristic of the automatically fabricated weld geometry is of greater significance. The present weld geometry is characterised by a very mild notch for the brace to weld transition and a comparatively sharp notch for the chord to weld transition (2), respectively. This characteristics lead to an enlarged elastic fatigue notch factor K_f as well as equivalent SCF_{NSA} for the chord sided notch which are significantly increased compared to the SCF values based on the SSA. Therefore, the prediction of the location for crack initiation varies between both approaches

for these axially loaded tubular X-joints. The SSA predicts the brace sided notch as being more fatigue prone and the NSA goes for the chord sided notch.
Comparing these numerical results in Fig. 5 to the experimental investigations in Fig. 4 only the NSA is able to predict the correct location of crack initiation at the chord sided notch due to the consideration of the elastic fatigue notch factor K_f compared to the structural stress σ_{HS} for the SSA.

5 CONCLUSIONS

Within this publication the automatically welding procedure of tubular X-joints for jacket substructures of offshore wind energy turbines was presented. Additionally, the test setup to perform axial fatigue tests for the robot welded X-joints was explained focusing on the detection of the initial technical fatigue crack location. For the axially loaded X-joints the initial crack occurred within the chord sided notch close to the saddle position which was detected by applying the digital image correlation system ARAMIS. Within the brace sided notch no measurable fatigue damage occurred for the typical weld geometry of the automatically welded tubular X-joints.
The detected location of the technical crack was then compared to the numerical investigations applying the structural stress approach (SSA) as well as the notch stress approach (NSA). The outcomes of these analyses indicate that the SSA is not able to determine the fatigue prone notch of the automatically welded tubular X-joint correctly due to the considered structural stress. In contrast, the NSA is able to accurately determine the hot spot of the fatigue effective stress and hence the correct location of the technical crack for the axially loaded X-joints due to the computed notch stress. This justifies the larger numerical modeling effort required for the application of the NSA.
In total 32 axial fatigue tests will be performed in future to determine S-N curves for automatically welded tubular joints whereby 16 X-joints will have an inner root layer included.

ACKNOWLEDGEMENT

The results are developed within the German FOSTA joint research project ‘FATInWeld’ supported via AiF (IGF 19104 N) within the programme for promoting the Industrial Collective Research (IGF) of the German Ministry of Economic Affairs and Energy (BMWi), based on a resolution of the German Parliament. The authors express their deep gratitude for the financial support received from the BMWi, the AiF and the FOSTA as well as from the companies involved in the project.

REFERENCES

1. *Salzgitter Supply Chain Concept for Industrial Assembling of Offshore-Wind-Jackets.* **Michels, Georg and Stephan, Brauser.** Hannover : Conference Proceedings of the International Wind Engineering Conference Hannover, 2014.
2. **Schaumann, Peter, et al., et al.** Automated Manufacturing of Tubular Joints for Jacket Support Structures - Description of the Welding Process Chain as well as Integration of the Process Parameters within the Fatigue Design. *Stahlbau.* 2018, Vol. 87, 9, pp. 897 - 909.
3. DIN EN 10210. *Hot finished structural steel hollow sections - Part 1: General; German and English version.* s.l. : Beuth Verlag, 2016.
4. ISO 14341 . *Welding consumables - Wire electrodes and weld deposits for gas shielded metal arc welding of non alloy and fine grain steels - Classification.* s.l. : International Organization for Standardization, 2010.
5. **Neubert, S., Pittner, Andreas and Rethmeier, Michael.** Influence of non-uniform martensitic transformation on residual stresses and distortion of GMA-welding. *Journal of Constructional Steel Research.* 2017, Vol. 128, pp. 193-200.
6. DNVGL-RP-C203 . *Fatigue Design of Offshore Steel Structures.* s.l. : DNV GL AS, 2016.
7. **Hobbacher, A.** *Recommendations for fatigue design of welded joints and components.* s.l. : IIW Document No. IIW-1823-07, International Institute of Welding, 2016.
8. **Schaumann, Peter and Schürmann, Karsten.** New proposal to express notch stress approach results by equivalent SCFs. *International Journal of Fatigue.* 2019, Vol. 119, pp. 11-19.